Cell. Mol. Biol. (ISSN: 1165-158X)

Journal Homepage: www.cellmolbiol.org

Cellular and Molecular Biology

Original Article

Mitochondria-targeted reactive oxygen species blockor SS-31 blocks hepatic stellate cell activation and alleviates hepatic fibrosis by regulating NLRP3 inflammasomes

Li Liu, YingFeng Wei, NingSheng Xie, Hong Cai, Ye Lin*

Department of Gastroenterology, Ganzhou People's Hospital, Ganzhou City, 341000, China

Article Info

Article history:

Received: September 15, 2023
Accepted: December 12, 2023
Published: February 29, 2024

Use your device to scan and read the article online

Abstract

This study aimed to elucidate the effect of mitochondria-targeted reactive oxygen species (ROS) blockor SS-31 on hepatic stellate cells (HSC) activation during liver fibrosis. TGF-β1 was employed to induce HSC activation, while MitoSOX Red was utilized to assess the presence of mitochondrial ROS. The mitochondrial membrane potential (MMP) was measured using the JC-1 probe, and the ATP level was determined using a specific kit. The proliferation of HSCs was assessed using CCK-8 and colony formation assays, whereas flow cytometry was employed to detect HSC apoptosis. Fibrotic markers (COL1A1 and α-SMA) and NLRP3 inflammasome components (NLRP3, caspase-1, and ASC) were analyzed via Western blotting. Liver fibrosis was induced in mice using CCl4, and subsequently, histopathological changes were observed through HE staining and Masson staining. In TGF-β1-activated HSCs, mitochondrial ROS expression increased, MMP and ATP content decreased, indicating mitochondrial damage. After TGF-β1 induction, HSC proliferation increased, apoptosis decreased, and COL1A1, α-SMA, and NLRP3 inflammasome protein expression increased. After SS-31 treatment, mitochondrial ROS expression decreased, MMP recovered, ATP level increased, HSC proliferation decreased, apoptosis increased, and the expressions of COL1A1, α-SMA, and NLRP3 inflammasome decreased. NLRP3 blockor MCC950 treatment blocked HSC activation. CCL4-induced liver fibrosis mice had inflammatory cell infiltration and significant collagen fiber deposition in the liver. After SS-31 treatment, liver inflammation and collagen deposition were significantly reduced. SS-31, as a mitochondria-targeted ROS blockor, can block HSC activation by regulating the NLRP3 inflammasome, thereby alleviating liver fibrosis.

Keywords: Hepatic stellate cells, Liver fibrosis, SS-31, Mitochondria-targeted ROS blockor, NLRP3 inflammasome.

1. Introduction

In liver fibrosis, abnormal connective tissue proliferation and excessive extracellular matrix accumulation occur as the result of various pathogenic factors. Liver fibrosis commonly develops in chronic liver diseases such as autoimmune hepatitis, hepatitis B and C, alcoholic liver disease, non-alcoholic liver disease, and cholestasis [1, 2]. Liver fibrosis can progress to cirrhosis, liver failure, and liver cancer if left untreated [3]. Approved drugs are far-fetched for liver fibrosis, despite its increasing morbidity and mortality rates [4].

A key step in liver fibrosis is hepatic stellate cell (HSCs) activation. As soon as resident HSCs are activated, they manifest as fibrogenic myofibroblasts, which produce large quantities of extracellular matrix proteins, including collagen 1, so that liver fibrosis ensues. A range of growth factors and cytokines stimulate HSC activation, including TGF-β [5, 6]. For this reason, blocking HSC activation may prove beneficial in treating liver fibrosis.

A multi-protein complex called NLRP3 inflammasome is expressed by both hepatic parenchymal and nonparenchymal cells [7, 8]. In normal circumstances, NLRP3 inflammasome is inactive. NLRP3 inflammasome activates in response to danger signals and interacts with pro-caspase 1 and ASC. NLRP3 inflammasome activation triggers the cleavage and activation of pro-caspase 1, subsequently enhancing the maturation of proinflammatory factors and leading to proinflammatory reactions [9]. Activation of inflammasomes has been implicated in liver diseases, including NASH and fibrogenesis [10, 11]. There is evidence that NLRP3 inflammasome activates HSCs and promotes fibrosis development [12].

In hepatocytes, mitochondria are the primary energy source and are essential for the normal function of the liver. For ATP synthesis, electrons are transported by the electron transport chain (ETC) and mitochondrial membrane potential (MMP) is generated. There is a possibility that some electrons may escape and generate ROS [13, 14]. ROS promotes HSC activation [15-17], and intracellular ROS can cause NLRP3 inflammasome activation [18-20].

An aromatic cationic peptide, Szeto-Schiller (SS)-31 peptide, scavenges hydrogen peroxide, superoxide,

* Corresponding author.
E-mail address: m13576799339@163.com (Y. Lin).
Doi: http://dx.doi.org/10.14715/cmb/2024.70.2.25

hydroxyl radicals, and peroxynitrite exclusively from mitochondrial inner membranes [21]. In epithelial, endothelial, and neuronal cells stimulated with pro-oxidants and ETC blockers, SS-31 decreases mitochondrial ROS [22, 23]. SS-31 is effective when administered to animal models that have mitochondrial oxidative stress, including ischemic brain injury [24], neurotoxicity [25], and excess fat intake-induced insulin resistance [26]. However, until now, the role of SS-31 in liver fibrosis has been unclear.

Therefore, this study was to investigate SS-31 in liver fibrosis. In this study, SS-31 blocks HSC activation by NLRP3 inflammasomes, thereby alleviating liver fibrosis. These results may provide a new approach for the treatment of liver fibrosis.

2. Materials and methods

2.1. Cell culture and treatments

LX-2 HSCs (Cell Center, Shanghai Academy of Biological Sciences, Shanghai, China) were cultured with DMEM (Gibco, Rockville, MD, USA) containing 10% FBS and 1% streptomycin/penicillin (Gibco, Rockville, MD, USA). TGF-β1 (10 ng/mL) was added to serum-free DMEM to activate LX-2 cells for 24 h. LX-2 cells were pretreated with SS-31 (50 μM) or the NLRP3 blockor MCC950 (1 μM) to explore the regulatory mechanism of SS-31 on HSC activation.

2.2. Mitochondrial ROS detection

The probe (5 μm, Beyotime, Shanghai, China) was added to HSCs and detected avoiding light. After PBS washing, HSCs were stained with 10 μg/ml Hoechst33342 solution (Beyotime, Shanghai, China), and viewed under a fluorescence microscope (DMI3000B, Leica Corporation, Wetzlar, Germany).

2.3. MMP detection

MMP was measured by a JC-1 probe (Beyotime, Shanghai, China). Simply put, HSCs were treated with JC-1 probe, and the nucleus was then observed in the dark with DAPI staining (Beyotime, Shanghai, China). An analysis of the red-green fluorescence intensity of the JC-1 probe was conducted.

2.4. ATP measurements

ATP in HSCs was detected by the assay kit (Beyotime, Shanghai, China) as required by the manufacturer's protocol.

2.5. CCK-8 assay

LX-2 cells were put in 96-well plates at 5×10^3 cells/well at 37°C under 5% CO_2. At days 1, 2, and 3, cells were detected with 10 μl CCK-8 reagent in each well (Shanghai Obio Technology, Shanghai, China) for 4 h. Using a microplate reader (Bio-Tek Instruments, Biotek Winooski, VT, USA), optical density at 450 nm was quantified.

2.6. Colony formation experiment

LX-2 cells were cultured in 6-well plates at 1000 cells per well. Over a span of 14 days, the culture medium was replaced every three days. Subsequently, the colonies were immobilized using a 4% paraformaldehyde solution and subjected to staining with crystal violet for a duration of 30 min. A quantitative assessment was conducted to determine the number of colonies consisting of more than 50 cells.

2.7. Flow cytometry

Apoptosis was assessed through flow cytometry utilizing a cell cycle and apoptosis assay kit (Beyotime, Shanghai, China). Specifically, the cells were immobilized with 70% ethanol and subjected to staining with 0.5 mL of propidium iodide (PI) staining buffer (200 mg/mL RNase A + 50 μg/mL PI) at 37°C for a duration of 30 min in the absence of light. Subsequently, analysis was conducted using the BD LSR flow cytometer (BD Biosciences, San Jose, CA, USA) and the number of apoptotic cells was quantified.

2.8. Animal experiment

Male SPF-grade C57BL/6 mice (6-8 weeks old, 20 ± 2 g) were purchased from SLAC Laboratory Animal Co., Ltd (Shanghai, China) and raised in the SPF animal room. There were five mice in each cage (20-25°C, 40-70% humidity) and they had enough food and water. The Animal Experiment Ethics and Welfare Committee of Ganzhou People's Hospital granted approval for all animal experiments conducted. After 1-week adaptive feeding, carbon tetrachloride (CCl4) diluted by vegetable oil at 1:4 was injected subcutaneously at 5 ml/kg into mice twice a week for 6 weeks. The Sham group consisted of mice that were solely injected with vegetable oil. To investigate the regulatory effect of SS-31, mice were injected with 3 mg/kg SS-31 (China Peptides Co., Ltd., Shanghai, China) subcutaneously, once a day for 6 weeks. There was Sham group, CCl4 group, and CCl4 + 3 mg/kg SS-31 group, with 6 mice in each group.

2.9. Serum biochemical analysis

Approximately 500 μl of blood was collected from the mouse eyeball and left to stand in centrifuge tubes at room temperature for a duration of 1-2 hours. Subsequently, the tubes were subjected to centrifugation at 4°C and 3,000 rpm for a period of 10 min, resulting in the collection of serum. The harvested serum was either transferred to a centrifuge tube or stored at -80°C. The analysis of serum ALT and AST levels was conducted using assay kits (Nanjing Jiancheng, Nanjing, China).

2.10. HE staining

Liver tissue was dehydrated with gradient-concentration ethanol, and immersed in paraffin, and the section thickness was 5 μm. The sections underwent dewaxing using xylene, followed by treatment with ethanol and immersion in distilled water. Hematoxylin was subsequently introduced and allowed to react for a duration of 10 min. The sections were then differentiated using a 5% acetic acid solution for 30 s, stained with a 1% eosin solution for 5 min, dehydrated, permeabilized, mounted, and finally observed under an optical microscope manufactured by Olympus (Tokyo, Japan).

2.11. Masson staining

The liver tissue paraffin sections underwent dewaxing and hydration, followed by staining with Weigert hematoxylin iron stain (Beyotime, Shanghai, China) for a duration of 5 min. Subsequently, the sections were treated with 1% hydrochloric acid alcohol for 10 s, rinsed with running water, and stained with Ponceau acid fuchsin solution

for 10 min. Aniline blue solution was then applied to the sections for 5 min, followed by treatment with 1% glacial acetic acid for 1 min and dehydration with ethanol. The sections were examined under an optical microscope (Olympus, Tokyo, Japan) after undergoing penetration and quenching.

2.12. Western blot

The total protein of HSCs or tissues was extracted using radioimmunoprecipitation assay (RIPA) lysis buffer and assayed by bicinchoninic acid (BCA) kit (Shanghai Jining Biotechnology Co., LTD., Shanghai, China). A 30 μg protein sample was separated by 12% sodium dodecyl sulphate-polyacrylamide gel electrophoresis (SDS-PAGE), and then wet transferred to nitrocellulose membranes (GE Healthcare, Little Chalfont, Buckinghamshire, UK). Subsequently, the membrane was closed with 5% skim milk for 2 h and detected with COL1A1 (1:2000, ab260043, Abcam, Cambridge, MA, USA), α-SMA (1:5000, ab124964, Abcam, Cambridge, MA, USA), NLRP3 (1:1000, 15101, Cell Signaling Technology, Danvers, MA, USA), Caspase-1 (1:1000, ab179515, Abcam, Cambridge, MA, USA), ASC (1:1000, 67824, Cell Signaling Technology, Danvers, MA, USA), and GAPDH (1:1000, 41549, Cell Signaling Technology, Danvers, MA, USA) at 4°C overnight. Then, the membrane was combined with a secondary anti-rabbit antibody at room temperature for 1 h, on which protein signals were visualized using electrochemiluminescence (ECL) Plus (Solarbio, Beijing, China) and analyzed using ImageJ.

2.13. Statistical analysis

All data were demonstrated as mean ± SEM and statistically analyzed by Statistic Package for Social Science (SPSS) 22.0 (IBM, Armonk, NY, USA). Differences between groups were compared using the Student t-test, while those between multiple groups were compared using the one-way analysis of variance. $P < 0.05$ was considered statistically significant.

3. Results

3.1. SS-31 can ameliorate TGF-β1-activated HSC mitochondrial dysfunction

Mitochondrial ROS levels increased (Figure 1A) and MMP and ATP content decreased (Figure 1B, 1C) in TGF-β1-activated LX-2 cells, suggesting mitochondrial damage. To determine SS-31's action in HSC activation, activated LX-2 cells were treated with 50 μM SS-31. After SS-31 treatment, mitochondrial ROS in HSCs was reduced (Figure 1A), MMP was restored (Figure 1B), and ATP content was increased (Figure 1C).

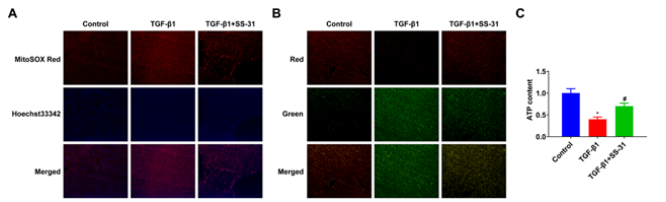

Fig. 1. SS-31 can improve TGF-β1-activated mitochondrial dysfunction of HSCs. (A) MitoSOX Red fluorescence images (the heavier the red, the more damage); (B) JC-1 fluorescence images (the more JC-1 monomers with green, the more damage to mitochondria); (C) ATP content; Data are expressed in mean ± SD; * $P < 0.05$ *vs.* Control group; # $P < 0.05$ *vs.* TGF-β1 group.

3.2. SS-31 can block HSC proliferation induced by TGF-β1 and enhance cell apoptosis

Subsequently, LX-2 cell proliferation was assessed using CCK-8 and colony formation assay, revealing that the administration of SS-31 effectively inhibited the proliferative capacity of LX-2 cells (Figure 2A-2C). Flow cytometry analyzed the apoptosis of LX-2 cells, and it was found that LX-2 cell apoptosis rate increased after SS-31 treatment (Figure 2D, 2E).

3.3. SS-31 alleviates TGF-β1-activated HSC fibrosis

The fibrosis markers, COL1A1 and α-SMA, were assessed using Western blot analysis. Following treatment with SS-31, COL1A1 and α-SMA proteins in LX-2 cells exhibited a decrease (Figure 3A, 3B), indicating that SS-31 possesses the ability to mitigate TGF-β1-induced fibrosis in HSCs.

3.4. SS-31 blocks HSC activation by regulating NLRP3 inflammasomes

To explore the potential mechanism of SS-31 blocking HSC activation, NLRP3 inflammasomes (NLRP3, caspase-1, and ASC) were assayed by Western blot analysis. The three indicators were downregulated in LX-2 cells after SS-31 conditioning (Figure 4A, 4B). In addition, similar to SS-31 treatment, treatment with the NLRP3 blockor MCC950 blocked HSC activation (Figure 5A-5G).

3.5. SS-31 can alleviate liver injury and fibrosis in mice

CCl4 was used to induce liver fibrosis in mice, while the mice were injected with 3 mg/kg SS-31. Then, serum

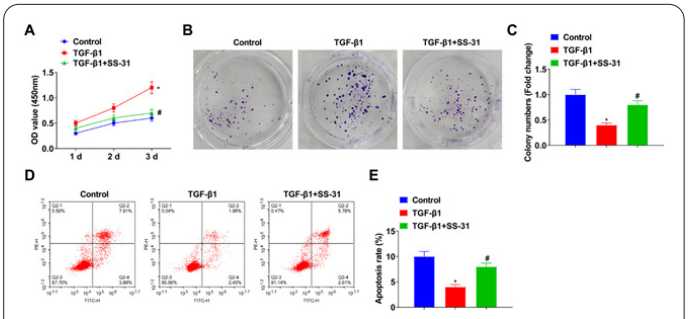

Fig. 2. SS-31 can block the proliferation of HSCs induced by TGF-β1 and promote cell apoptosis. (A) CCK-8 detected cell proliferation; (B-C) Colony formation assay detected cell proliferation; D-E: Flow cytometry detected apoptosis. Data are expressed in mean ± SD; * $P < 0.05$ *vs.* Control group; # $P < 0.05$ *vs.* TGF-β1 group.

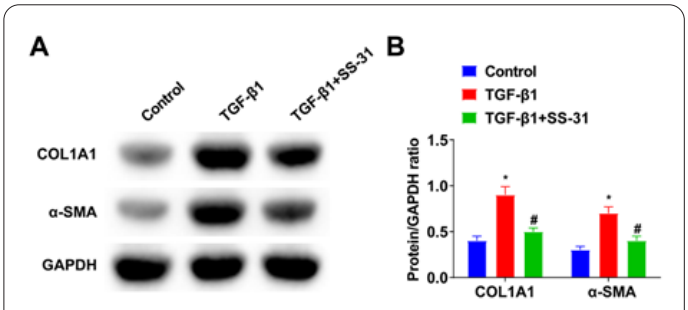

Fig. 3. SS-31 alleviates TGF-β1-activated HSC fibrosis. (A-B) Western blot measured fibrosis markers (COL1A1 and α-SMA). Data are expressed in mean ± SD; * $P < 0.05$ *vs.* Control group; # $P < 0.05$ *vs.* TGF-β1 group.

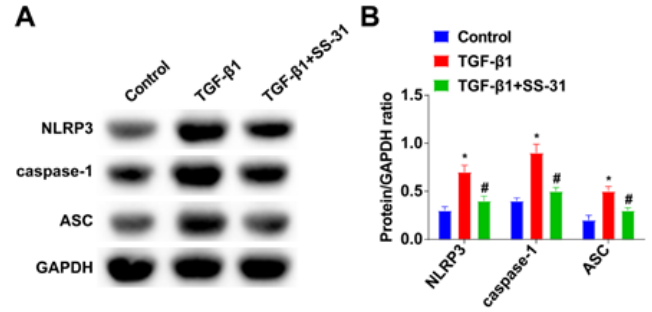

Fig. 4. SS-31 blocks HSC activation by regulating NLRP3 inflammasomes. (A-B) Western blot analysis of NLRP3 inflammasomes (NLRP3, caspase-1, and ASC); Data are expressed in mean ± SD; * $P < 0.05$ *vs.* Control group; # $P < 0.05$ *vs.* TGF-β1 group.

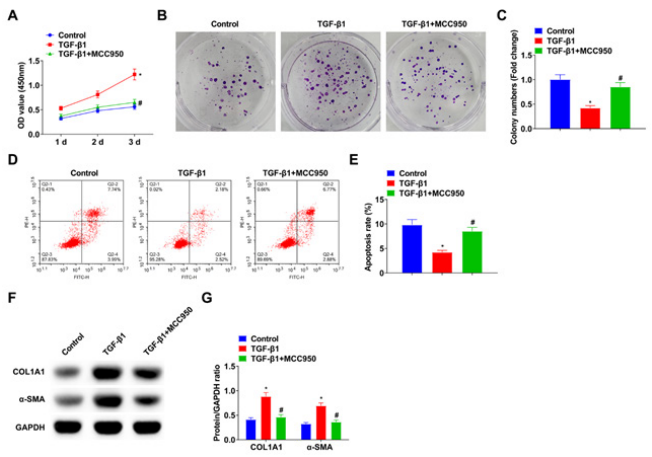

Fig. 5. Treatment with NLRP3 blockor MCC950 can block HSC activation. (A) CCK-8 detected cell proliferation; (B-C) Colony formation assay detected cell proliferation; (D-E) Flow cytometry detected apoptosis; (F-G) Western blot detected fibrosis markers (COL1A1 and α-SMA). Data are expressed in mean ± SD; * $P < 0.05$ *vs.* Control group; # $P < 0.05$ *vs.* TGF-β1 group.

ALT and AST of mice were quantified, and the results demonstrated that serum AST and ALT of mice with liver fibrosis were increased, and decreased after SS-31 treatment (Figure 6A, 6B). The liver stained with HE had a large number of inflammatory cells infiltrated in fibrotic mice (Figure 6C), and Masson staining found significant collagen fiber deposition (Figure 6D). After SS-31 treatment, liver inflammatory damage and collagen deposition were alleviated (Figure 6A, 6B).

4. Discussion

Our study confirms that SS-31 treatment mitigated mitochondrial damage and NLRP3 inflammasome activation, blocked HSC activation and alleviated liver damage and fibrosis.

A pro-fibrotic cytokine, TGF-1, can induce extracellular matrix production [27]. This study established a TGF-β1-activated LX2 cell model, which has been studied in liver fibrosis [28]. In this study, HSCs were stimulated with TGF-β1 at 10 ng/mL. A well-known fact is that activated HSCs are the main source of stroma-secreting myofibroblasts that cause liver fibrosis [29]. In an activated state, the proliferation capacity of HSCs is promoted, and apoptosis is reduced [30]. Our results showed that SS-31 could block the proliferation of TGF-β1-activated LX2 cells and promote cell apoptosis, suggesting that SS-31 could effectively block HSC activation. As HSCs are activated, they transform into myofibroblasts, undergo morphological alteration, form extracellular matrix massively, and express α-SMA. As collagen builds up in the extracellular matrix, it is thought that collagen represents liver fibrosis progress or regression [31]. This research demonstrated that SS-31 lowered COL1A1 and α-SMA.

Different chronic and acute liver diseases have been linked to NLRP3 inflammasome activation, causing liver damage and fibrosis [8]. The findings of our study provide confirmation that there was an increase in NLRP3 inflammasome protein in activated HSCs. It is widely accepted that ROS serves as the primary trigger for NLRP3 inflammasome activation [32], consequently promoting the development of chronic inflammation and fibroplasia. This activation of HSCs ultimately leads to the progression of fibrosis [33, 34]. Furthermore, the induction of oxidative stress plays a substantial role in HSC activation and fibrosis [35]. This study analysis confirmed an increase in mitochondrial ROS production in activated HSCs. The reduction of oxidative stress and elimination of ROS are, therefore, promising therapeutic strategies for treating liver fibrosis.

Under multiple conditions, SS-31 can reduce mitochondrial ROS production, improve ATP production, and interact with mitochondrial cardiolipin, decreasing oxidative stress [36,37]. Antioxidant properties of SS-31 have been applied to treat Alzheimer's disease [38], atherosclerosis [39], and ischemia-reperfusion injury [40]. In this study, SS-31 treatment reduced mitochondrial ROS production and down-regulated NLRP3 inflammasome protein expression, thereby alleviating liver fibrosis.

The subcutaneous injection of CCl4 has proven to be effective in inducing histological changes resembling human liver disease, as well as elevating serum ALT levels. The occurrence of fibrosis in the liver can be attributed to the persistent injury of hepatic cells, excessive deposition of extracellular matrix (ECM), and abnormal proliferation of connective tissue within the liver [41]. In this study, serum AST and ALT levels were elevated in mice with liver fibrosis and decreased after SS-31 treatment. Following administration of SS-31, mice with liver fibrosis exhibited mitigated liver inflammation damage and reduced collagen deposition. In summary, SS-31 mitigated liver injury and fibrosis in mice.

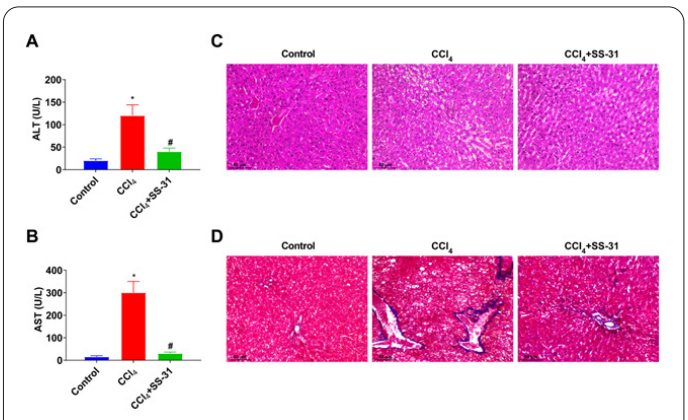

Fig. 6. SS-31 alleviates CCL4-induced liver injury and liver fibrosis in mice. (A-B) Serum ALT and AST levels; (C) HE staining; (D) Masson dyeing; Data are expressed in mean ± SD; * $P < 0.05$ *vs.* Sham group; # $P < 0.05$ *vs.* CCl4 group.

5. Conclusion

In summary, SS-31 blocks HSC activation by blocking NLRP3 inflammasome activation and mitochondrial ROS production, thereby blocking liver injury and fibrosis. It is suggested that SS-31 may be an effective drug for liver fibrosis.

Competing interests

The authors have no conflicts of interest to declare.

Consent for publications

The author read and approved the final manuscript for publication.

Ethics approval

The animal experiments were approved by the Animal Committee of Ganzhou People's Hospital. All procedures complied with the National Institutes of Health Guide for the Use of Laboratory Animals.

Availability of data and materials

The datasets used and/or analyzed during the present study are available from the corresponding author upon reasonable request.

Informed consent

The authors declare not used any patients in this research.

Authors' contributions

L.L. designed the research study. L.L. and Y.W. performed the research. N.X. provided help and advice on the experiments. H.C. and Y.L. analyzed the data. L.L. and Y.L. wrote the manuscript. All authors contributed to editorial changes in the manuscript. All authors read and approved the final manuscript.

Funding

Jiangxi Provincial Youth Science Foundation Grant Project (20181BAB215006)

Acknowledgments

Not applicable.

References

1. Huang S, Qian X, Jiang T, Xiao J, Yin M, Xiong M et al (2022) Mechanism of dact2 gene inhibiting the occurrence and development of liver fibrosis. Cell Mol Biol 67:33-39. doi: 10.14715/cmb/2021.67.6.5
2. Seki E, Brenner DA (2015) Recent advancement of molecular mechanisms of liver fibrosis. J Hepato-Bil-Pan Sci 22:512-518. doi: 10.1002/jhbp.245
3. Aydin MM, Akcali KC (2018) Liver fibrosis. Turk J Gastroenterol 29:14-21. doi: 10.5152/tjg.2018.17330
4. Muriel P (2019) Fighting liver fibrosis to reduce mortality associated with chronic liver diseases: The importance of new molecular targets and biomarkers. Ebiomedicine 40:35-36. doi: 10.1016/j.ebiom.2019.02.002
5. Radaeva S, Sun R, Jaruga B, Nguyen VT, Tian Z, Gao B (2006) Natural killer cells ameliorate liver fibrosis by killing activated stellate cells in NKG2D-dependent and tumor necrosis factor-related apoptosis-inducing ligand-dependent manners. Gastroenterology 130:435-452. doi: 10.1053/j.gastro.2005.10.055
6. Ruan W, Pan R, Shen X, Nie Y, Wu Y (2019) CDH11 promotes liver fibrosis via activation of hepatic stellate cells. Biochem Bioph Res Co 508:543-549. doi: 10.1016/j.bbrc.2018.11.153
7. Xu L, Su J, Du C, Liu H, Lv W (2023) Ghrelin suppresses hypoxia/reoxygenation-induced H9C2 cell pyroptosis via NLRP3. Cell Mol Biol 69:196-202. doi: 10.14715/cmb/2023.69.13.30
8. Wree A, Eguchi A, McGeough MD, Pena CA, Johnson CD, Canbay A et al (2014) NLRP3 inflammasome activation results in hepatocyte pyroptosis, liver inflammation, and fibrosis in mice. Hepatology 59:898-910. doi: 10.1002/hep.26592
9. Takeuchi O, Akira S (2010) Pattern recognition receptors and inflammation. Cell 140:805-820. doi: 10.1016/j.cell.2010.01.022
10. Csak T, Ganz M, Pespisa J, Kodys K, Dolganiuc A, Szabo G (2011) Fatty acid and endotoxin activate inflammasomes in mouse hepatocytes that release danger signals to stimulate immune cells. Hepatology 54:133-144. doi: 10.1002/hep.24341
11. Henao-Mejia J, Elinav E, Jin C, Hao L, Mehal WZ, Strowig T et al (2012) Inflammasome-mediated dysbiosis regulates progression of NAFLD and obesity. Nature 482:179-185. doi: 10.1038/nature10809
12. Inzaugarat ME, Johnson CD, Holtmann TM, McGeough MD, Trautwein C, Papouchado BG et al (2019) NLR Family Pyrin Domain-Containing 3 Inflammasome Activation in Hepatic Stellate Cells Induces Liver Fibrosis in Mice. Hepatology 69:845-859. doi: 10.1002/hep.30252
13. Mansouri A, Gattolliat CH, Asselah T (2018) Mitochondrial Dysfunction and Signaling in Chronic Liver Diseases. Gastroenterology 155:629-647. doi: 10.1053/j.gastro.2018.06.083
14. Figueira TR, Barros MH, Camargo AA, Castilho RF, Ferreira JC, Kowaltowski AJ et al (2013) Mitochondria as a source of reactive oxygen and nitrogen species: from molecular mechanisms to human health. Antioxid Redox Sign 18:2029-2074. doi: 10.1089/ars.2012.4729
15. Kong M, Chen X, Lv F, Ren H, Fan Z, Qin H et al (2019) Serum response factor (SRF) promotes ROS generation and hepatic stellate cell activation by epigenetically stimulating NCF1/2 transcription. Redox Biol 26:101302. doi: 10.1016/j.redox.2019.101302
16. Ge C, Tan J, Lou D, Zhu L, Zhong Z, Dai X et al (2022) Mulberrin confers protection against hepatic fibrosis by Trim31/Nrf2 signaling. Redox Biol 51:102274. doi: 10.1016/j.redox.2022.102274
17. Lv F, Li N, Kong M, Wu J, Fan Z, Miao D et al (2020) CDKN2a/p16 Antagonizes Hepatic Stellate Cell Activation and Liver Fibrosis by Modulating ROS Levels. Front Cell Dev Biol 8:176. doi: 10.3389/fcell.2020.00176
18. Minutoli L, Puzzolo D, Rinaldi M, Irrera N, Marini H, Arcoraci V et al (2016) ROS-Mediated NLRP3 Inflammasome Activation in Brain, Heart, Kidney, and Testis Ischemia/Reperfusion Injury. Oxid Med Cell Longev 2016:2183026. doi: 10.1155/2016/2183026
19. Zhao K, Zhao GM, Wu D, Soong Y, Birk AV, Schiller PW et al (2004) Cell-permeable peptide antioxidants targeted to inner mitochondrial membrane inhibit mitochondrial swelling, oxidative cell death, and reperfusion injury. J Biol Chem 279:34682-34690. doi: 10.1074/jbc.M402999200
20. Cai SM, Yang RQ, Li Y, Ning ZW, Zhang LL, Zhou GS et al (2016) Angiotensin-(1-7) Improves Liver Fibrosis by Regulating the NLRP3 Inflammasome via Redox Balance Modulation. Antioxid Redox Sign 24:795-812. doi: 10.1089/ars.2015.6498
21. Szeto HH (2008) Mitochondria-targeted cytoprotective peptides for ischemia-reperfusion injury. Antioxid Redox Sign 10:601-619. doi: 10.1089/ars.2007.1892
22. Whiteman M, Spencer JP, Szeto HH, Armstrong JS (2008) Do mitochondriotropic antioxidants prevent chlorinative stress-induced mitochondrial and cellular injury? Antioxid Redox Sign 10:641-650. doi: 10.1089/ars.2007.1879
23. Zhao K, Luo G, Giannelli S, Szeto HH (2005) Mitochondria-tar-

geted peptide prevents mitochondrial depolarization and apoptosis induced by tert-butyl hydroperoxide in neuronal cell lines. Biochem Pharmacol 70:1796-1806. doi: 10.1016/j.bcp.2005.08.022
24. Cho S, Szeto HH, Kim E, Kim H, Tolhurst AT, Pinto JT (2007) A novel cell-permeable antioxidant peptide, SS31, attenuates ischemic brain injury by down-regulating CD36. J Biol Chem 282:4634-4642. doi: 10.1074/jbc.M609388200
25. Yang L, Zhao K, Calingasan NY, Luo G, Szeto HH, Beal MF (2009) Mitochondria targeted peptides protect against 1-methyl-4-phenyl-1,2,3,6-tetrahydropyridine neurotoxicity. Antioxid Redox Sign 11:2095-2104. doi: 10.1089/ars.2009.2445
26. Anderson EJ, Lustig ME, Boyle KE, Woodlief TL, Kane DA, Lin CT et al (2009) Mitochondrial H2O2 emission and cellular redox state link excess fat intake to insulin resistance in both rodents and humans. J Clin Invest 119:573-581. doi: 10.1172/JCI37048
27. Shrestha N, Chand L, Han MK, Lee SO, Kim CY, Jeong YJ (2016) Glutamine inhibits CCl4 induced liver fibrosis in mice and TGF-beta1 mediated epithelial-mesenchymal transition in mouse hepatocytes. Food Chem Toxicol 93:129-137. doi: 10.1016/j.fct.2016.04.024
28. Xu L, Hui AY, Albanis E, Arthur MJ, O'Byrne SM, Blaner WS et al (2005) Human hepatic stellate cell lines, LX-1 and LX-2: new tools for analysis of hepatic fibrosis. Gut 54:142-151. doi: 10.1136/gut.2004.042127
29. Higashi T, Friedman SL, Hoshida Y (2017) Hepatic stellate cells as key target in liver fibrosis. Adv Drug Deliver Rev 121:27-42. doi: 10.1016/j.addr.2017.05.007
30. Xu Z, Li T, Li M, Yang L, Xiao R, Liu L et al (2018) eRF3b-37 inhibits the TGF-beta1-induced activation of hepatic stellate cells by regulating cell proliferation, G0/G1 arrest, apoptosis and migration. Int J Mol Med 42:3602-3612. doi: 10.3892/ijmm.2018.3900
31. Kennedy P, Taouli B (2020) Collagen-targeted MRI contrast agent for liver fibrosis detection. Nat Rev Gastro Hepat 17:201-202. doi: 10.1038/s41575-020-0266-z
32. Scambler T, Jarosz-Griffiths HH, Lara-Reyna S, Pathak S, Wong C, Holbrook J et al (2019) ENaC-mediated sodium influx exacerbates NLRP3-dependent inflammation in cystic fibrosis. Elife 8:e49248. doi: 10.7554/eLife.49248
33. Dickie LJ, Aziz AM, Savic S, Lucherini OM, Cantarini L, Geiler J et al (2012) Involvement of X-box binding protein 1 and reactive oxygen species pathways in the pathogenesis of tumour necrosis factor receptor-associated periodic syndrome. Ann Rheum Dis 71:2035-2043. doi: 10.1136/annrheumdis-2011-201197
34. Chen Y, Zhao C, Liu X, Wu G, Zhong J, Zhao T et al (2019) Plumbagin ameliorates liver fibrosis via a ROS-mediated NF-small ka, CyrillicB signaling pathway in vitro and in vivo. Biomed Pharmacother 116:108923. doi: 10.1016/j.biopha.2019.108923
35. Lin L, Gong H, Li R, Huang J, Cai M, Lan T et al (2020) Nanodrug with ROS and pH Dual-Sensitivity Ameliorates Liver Fibrosis via Multicellular Regulation. Adv Sci 7:1903138. doi: 10.1002/advs.201903138
36. Szeto HH, Liu S, Soong Y, Wu D, Darrah SF, Cheng FY et al (2011) Mitochondria-targeted peptide accelerates ATP recovery and reduces ischemic kidney injury. J Am Soc Nephrol 22:1041-1052. doi: 10.1681/ASN.2010080808
37. Birk AV, Liu S, Soong Y, Mills W, Singh P, Warren JD et al (2013) The mitochondrial-targeted compound SS-31 re-energizes ischemic mitochondria by interacting with cardiolipin. J Am Soc Nephrol 24:1250-1261. doi: 10.1681/ASN.2012121216
38. Reddy PH, Manczak M, Yin X, Reddy AP (2018) Synergistic Protective Effects of Mitochondrial Division Inhibitor 1 and Mitochondria-Targeted Small Peptide SS31 in Alzheimer's Disease. J Alzheimers Dis 62:1549-1565. doi: 10.3233/JAD-170988
39. Zhang M, Zhao H, Cai J, Li H, Wu Q, Qiao T et al (2017) Chronic administration of mitochondrion-targeted peptide SS-31 prevents atherosclerotic development in ApoE knockout mice fed Western diet. Plos One 12:e0185688. doi: 10.1371/journal.pone.0185688
40. Cai J, Jiang Y, Zhang M, Zhao H, Li H, Li K et al (2018) Protective effects of mitochondrion-targeted peptide SS-31 against hind limb ischemia-reperfusion injury. J Physiol Biochem 74:335-343. doi: 10.1007/s13105-018-0617-1
41. Hernandez-Gea V, Friedman SL (2011) Pathogenesis of liver fibrosis. Annu Rev Pathol-Mech 6:425-456. doi: 10.1146/annurev-pathol-011110-130246